

A Practical Methodology for Short-Circuit Current Determination in Power Converter-Dominated DC Microgrids

Jonathan Wilson¹, David Corbet², Bertrand du Peloux², Kilian Drexler³, Ahmad Makkieh¹

¹Schneider Electric, United Kingdom

²Schneider Electric, France

³Fraunhofer Institute for Integrated Systems and Device Technology IISB, Germany

Corresponding author: Jonathan Wilson, jonathan.wilson@se.com

Speaker: Kilian Drexler, kilian.drexler@iisb.fraunhofer.de

Abstract

As the energy landscape evolves, Direct Current (DC) has become a key enabler for integrating renewable energy sources and supplying native DC loads. DC microgrids are expected to play a vital role in emerging systems, including industrial applications, by optimising energy exchanges among sources, loads, and machines. Despite this, understanding short-circuit currents presents significant technical challenges, complicating the selection and design of reliable protection schemes. This difficulty arises from the lack of comprehensive calculation standards and analytical methods for DC microgrids, and the highly diverse, topology-dependent behaviour of power converters. To address this gap, this paper proposes a practical methodology to determine short-circuit currents in DC microgrids with sufficient accuracy. The influence of sources and power converters is analysed, the general approach and conditions to consider are outlined, and relevant outputs are proposed in the context of emerging technologies.

1 Introduction

Short-circuit currents in DC systems differ significantly from those in traditional AC systems. This is in part due to the capacitive nature of DC systems and the types of short-circuit current sources that exist. It also stems from the architecture and behaviour of DC microgrids, where sources are typically distributed, most loads contribute to short-circuits due to their capacitances, and the dominant presence of power converters that can contribute to and influence the short-circuit current.

IEC 61660-1 [1] outlines analytical methods for calculating short-circuit currents in DC auxiliary systems. However, its applicability to emerging DC power systems is limited. It does not account for converters common in DC microgrids – such as buck, boost, single active bridge, and dual active bridge – nor for photovoltaic (PV) systems, which are increasingly deployed. Additionally, it lacks coverage of active LVDC voltage levels [2], earthing configurations, and three-wire systems. The standard also simplifies capacitor contributions by assuming an overdamped transient response, which can significantly reduce the accuracy of short-circuit current and Joule integral (I^2t) calculations. Consequently, if the actual capacitor response was underdamped, this could lead to inaccurate overcurrent protective device operation evaluations [3].

A practical approach for accurately determining short-circuit currents in DC microgrids is essential for safe system

design. Section 2 examines short-circuit behaviour, highlighting contributing sources and the significant role of power converters. Section 3 introduces practical modelling strategies compatible with commercial transient analysis tools. A realistic case study is presented in Section 4 using the proposed methodology. Finally, Section 5 concludes the paper and outlines directions for future work.

2 DC Short-Circuit Currents

2.1 Understanding short-circuit currents

Short-circuits must be cleared promptly, as they pose serious risks including electric shock, fire, equipment damage, system failure, and increased costs. Accurate short-circuit current calculation is therefore essential for system design, supporting the evaluation of installation requirements and the protection of both people and assets. For effective protection scheme development and equipment selection, the full range of prospective short-circuit currents must be considered.

The maximum current is primarily required for equipment selection and supports protection scheme design and selectivity assessments. The minimum current is critical for ensuring protective devices can detect and interrupt short-circuits within a specified time. Evaluating both extremes enables comprehensive selectivity analysis across the full range of expected conditions.

2.2 Short-circuit contributors

In DC microgrids, various sources can contribute to a short-circuit such as AC/DC converters including the AC supply system, DC/DC converters including the respective DC sources and loads, capacitors, PV systems, batteries, regenerative loads, and fuel cells. A DC microgrid is typically highly capacitive and therefore an initial large transient short-circuit current with high rate-of-rise ($\Delta i/\Delta t$) is common, followed by a steady-state contribution phase in which the current is repetitive. The current magnitude usually peaks in the transient phase and is lower in the steady-state phase.

2.3 Influence of power converters

2.3.1 Evolution of the short-circuit current

Several stages of a short-circuit current can occur when a power converter has internal filters and diodes, along with external voltage or current sources. The evolution typically involves an initial capacitor discharge, followed by inductor discharge and input-side in-feed [4]-[5], as shown in Fig. 1 with a non-isolated AC/DC converter.

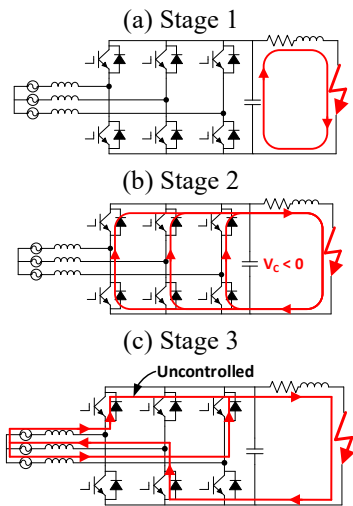


Fig. 1 Power converter short-circuit current evolution illustrated with a non-isolated AC/DC converter

Stage 1 occurs as capacitors are directly exposed to the short-circuit, resulting in a typically high current magnitude and rate-of-rise. This stage is energy-limited, dictated by the capacitor's stored energy. Stage 2 involves the free-wheeling of diodes due to energy stored in the loop inductance, including that from the discharged capacitor. This occurs only if the voltage goes negative and the diodes become forward biased, implying an underdamped response. Stage 3 involves the input source feeding the short-circuit, with the current eventually reaching a repetitive steady state. This stage is heavily influenced by the converter type, which affects both the magnitude and duration of the prospective short-circuit current – critical factors in protection and system safety.

2.3.2 Limiting and non-limiting type

Power converters exhibit diverse short-circuit behaviours depending on their topology and control strategy. These are generally categorised as limiting or non-limiting. In limiting converters, such as a buck converter, Stage 3 current can be controlled due to the absence of a direct freewheeling path between the input and the short-circuited output (see Fig. 2).

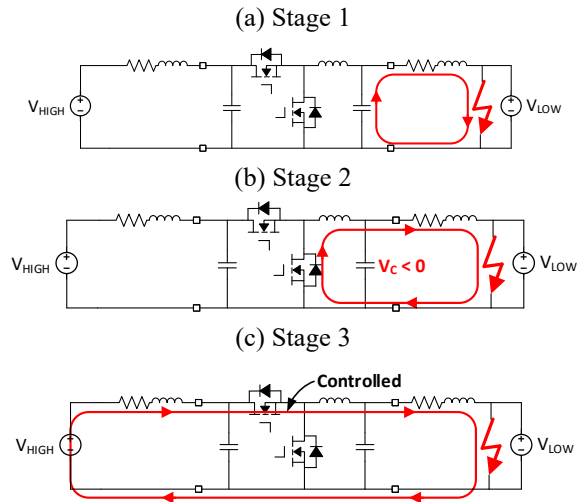


Fig. 2 DC/DC bidirectional buck/boost converter short-circuit current evolution (lower-voltage fault)

In contrast, non-limiting converters allow uncontrolled current flow from the input, governed by network and source conditions, due to the presence of a freewheeling path (see Fig. 1). Similarly, a short-circuit on the high-voltage side of the bidirectional buck/boost converter in Fig. 2 results in non-limiting behaviour, imposing severe stress on freewheeling components if not adequately protected.

Prospective short-circuit current waveforms of both types of converters are illustrated in Fig. 3. In each case, current continues to flow until overcurrent protective devices operate, the converter stops due to limits such as temperature, current, or voltage, or the energy sources are depleted.

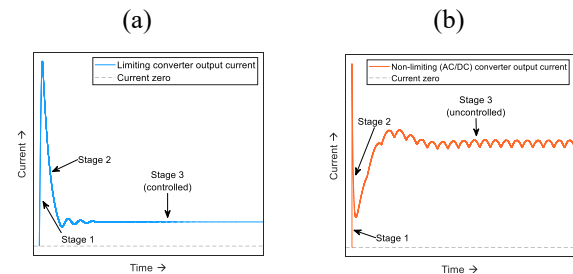


Fig. 3 Typical short-circuit current waveforms: (a) limiting converter; (b) non-limiting AC/DC converter

3 Methodology

3.1 General approach

It is important to apply appropriate methods when determining short-circuit currents to achieve sufficient accuracy while minimising expense. Given the limitations of IEC 61660-1 and the lack of validated analytical techniques for DC microgrids, this paper adopts a time-domain simulation approach (solving ordinary differential equations). It uses simplified behavioural models of power system components, including power converters. The overall methodology is outlined in Fig. 4, noting that Step 5 is beyond the scope of this paper.

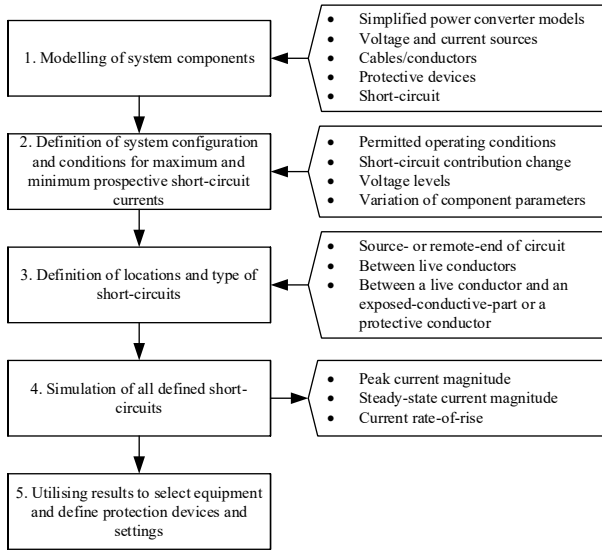


Fig. 4 High-level methodology summary

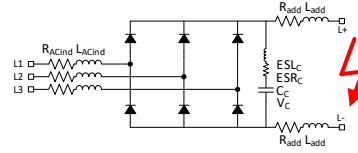
While this approach has limitations – including the need for, and proficiency in, transient analysis tools, calculation time, and manual post-processing of data – it is considered the most practical solution. It offers sufficient accuracy and supports rapid, widespread adoption via commercial software. Highly detailed component models are generally impractical, primarily due to the complexity of power converters which dominate DC microgrid architectures.

3.2 Behaviour and modelling

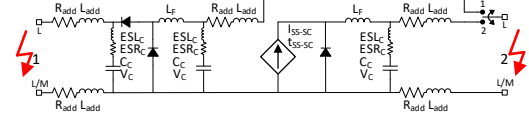
3.2.1 Power converters

As shown, power converters can both contribute to, and influence, short-circuit currents. Accurately predicting their full behaviour requires extensive knowledge of the internal design, including the control loops and protection mechanisms, which is often impractical. Therefore, this paper proposes simplified behavioural models based on the basic topologies of common non-isolated and isolated converters used in DC microgrids to estimate their short-circuit response (see Fig. 5). Models of this kind can also be extended to incorporate a distributed mid-point, enabling their application in three-wire systems.

(a) AC/DC non-isolated InterLink 2-level



(b) DC/DC non-isolated buck or boost (bidirectional)



(c) DC/DC isolated Single or Dual Active Bridge

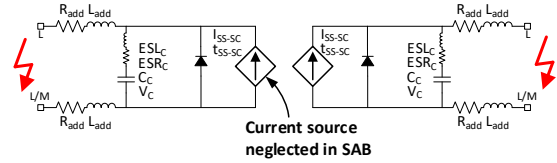


Fig. 5 Simplified short-circuit models: Examples for power converter topologies

For both maximum and minimum prospective short-circuit current determination, converters are assumed healthy with no faulty components. All models include passive components. The respective parameters are: R_{ACind} and L_{ACind} for the AC inductor resistance and inductance, L_F for the DC filter inductance, and R_{add} and L_{add} for the additional resistance and inductance up to the converter terminals. These latter parameters are particularly important for short-circuits occurring in close proximity to the converter. Capacitor parameters are as defined in Section 3.2.2.2.

The Stage 3 limiting behaviour of a converter is modelled using an ideal current source, with parameters I_{SS-SC} and t_{SS-SC} describing the steady-state short-circuit current output and duration, respectively. However, a limiting converter may embed self-protection techniques, such as "fold-back" (see Fig. 6a), reducing output current well below the rated maximum. Moreover, it may stop delivering current if the voltage reaches a minimum threshold. This concept of self-protection can be represented in simplified models by using a voltage-dependent current source with a defined output voltage-current profile as in Fig. 6b.

(a) (b)

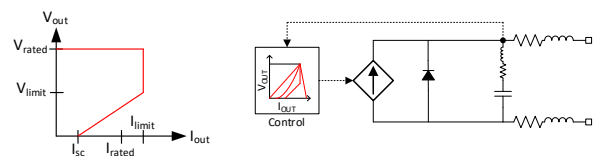


Fig. 6 Limiting converter: (a) Typical "fold-back" output current profile; (b) simplified modelling method

This behaviour is especially critical when evaluating minimum short-circuit currents and ensuring protective device sensitivity (see Fig. 7), considering that the voltage at each

limiting converter may vary depending on their location relative to the short-circuit and other sources – particularly constant voltage sources or supercapacitors capable of temporarily sustaining voltage – connected within the network.

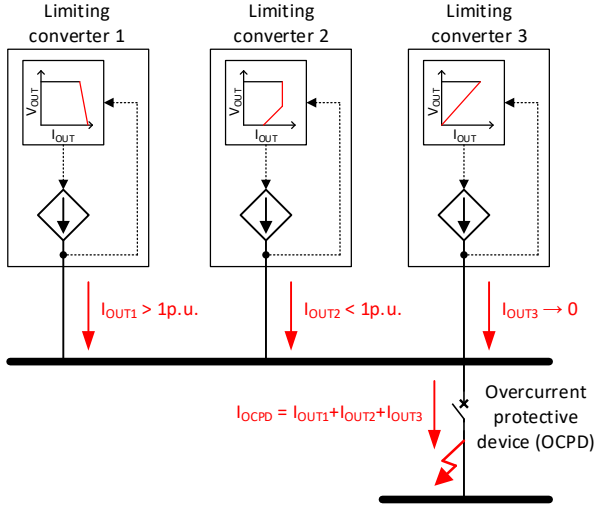


Fig. 7 Illustration of limiting converter behaviour and impact on the Stage 3 short-circuit current

3.2.2 Voltage sources

3.2.2.1 Batteries

Although various models exist [6], a battery can be modelled as a DC voltage source behind an impedance (see Fig. 8). The internal resistance (R_{BAT}) and inductance (L_{BAT}), accounting for cells, modules, and interconnections, are considered. Moreover, the state-of-charge prior to the short-circuit influences the current through its effect on the pre-fault voltage level, defined by the nominal open-circuit battery voltage, U_{BAT} , and voltage factor, c_{BAT} .

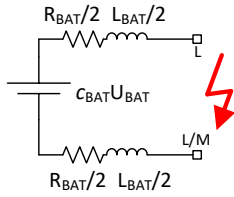


Fig. 8 Simplified short-circuit model: Battery

The short-circuit contribution may decline over time depending on the initial state-of-charge, energy capacity, and temperature dependency. These effects may require special consideration for minimum short-circuit current calculations.

3.2.2.2 Capacitors

Capacitors can be a dedicated component connected to a main bus and can be present in loads and converters. They are considered as a series-connected resistor-inductor-capacitor circuit. The resistor represents the Equivalent Series Resistance (ESR_C). The inductor represents the Equivalent Series Inductance (ESL_C). The ESL is often neglected as the external connections and network usually dominate

the loop inductance. In this model (see Fig. 9), the capacitance, C_C , is initially charged to a voltage, V_C .

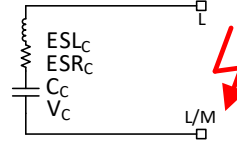


Fig. 9 Simplified short-circuit model: Capacitor

3.2.2.3 AC supply systems

AC systems can contribute to DC short-circuits via AC/DC converters. Since either the AC or DC side may be earthed, the AC system must be modelled to reflect both balanced and unbalanced conditions. For short-circuit analysis, the AC system is represented as a voltage source, with frequency f_n , behind an impedance. To align with IEC 60909 utilising symmetrical component concepts [7], the AC system impedance is modelled in the sequence domain, involving a mutual-coupling element with specified sequence impedances (see Fig. 10).

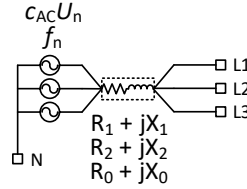


Fig. 10 Simplified short-circuit model: AC supply

In some cases, a power-frequency transformer external to the AC/DC converter provides galvanic isolation, with system earthing implemented on the DC side. Therefore, the AC supply can be modelled using only the positive-sequence impedance. For AC systems far from generators, the positive- and negative-sequence impedances are equal ($Z_1 = R_1 + jX_1 = Z_2$) and can be determined from the nominal line voltage, U_n , voltage factor, c_{AC} , three-phase initial symmetrical short-circuit current at the AC/DC converter input, I''_{k3} , and the corresponding X/R ratio, $(X/R)_{k3}$, as shown in Eqs. (1)-(3).

$$Z_1 = R_1 + jX_1 = \frac{c_{AC} \cdot U_n}{\sqrt{3} \cdot I''_{k3}} = Z_2 \quad (1)$$

$$R_1 = \frac{Z_1}{\sqrt{1 + (X/R)_{k3}^2}} = R_2 \quad (2)$$

$$X_1 = R_1 \cdot (X/R)_{k3} = X_2 \quad (3)$$

If the AC system is earthed, the zero-sequence impedance ($Z_0 = R_0 + jX_0$) can be determined from the initial line-to-earth short-circuit current at the AC/DC converter input, I''_{k1} , and the corresponding X/R ratio, $(X/R)_{k1}$, as shown in Eqs. (4)-(7). Equation (7) can be similarly applied for R_0 and X_0 .

$$Z_1 + Z_2 + Z_0 = Z_t = \frac{c_{AC} \cdot U_n \cdot \sqrt{3}}{I''_{k1}} \quad (4)$$

$$R_t = \frac{Z_t}{\sqrt{1 + (X/R)_{k1}^2}} \quad (5)$$

$$X_t = R_t \cdot (X/R)_{k1} \quad (6)$$

$$Z_0 = Z_t - 2 \cdot Z_1 \quad (7)$$

3.2.3 Current sources

Under short-circuit conditions, PV systems behave as current sources, typically delivering currents only slightly above normal levels. According to IEC 60364-7-712 [8], the maximum short-circuit current of a PV array is calculated as $I_{SC\ MAX} = K_I I_{SC\ STC}$, where K_I is a factor with a minimum value of 1.25 and $I_{SC\ STC}$ is the short-circuit current under standard test conditions. This approach is adopted in the model, which represents the PV array as a current source (see Fig. 11). While not part of the short-circuit model, the open-circuit voltage of the PV array ($U_{OC\ ARRAY}$) is relevant for specifying the voltage of the PV-side converter capacitors.

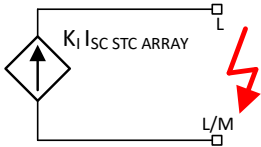


Fig. 11 Simplified short-circuit model: PV system

3.2.4 Passive components

3.2.4.1 Power circuits

Power cable and busway conductors influence the short-circuit current, primarily due to their overall resistance and inductance. IEC 61660-1 [1] considers a fixed-parameter series resistor-inductor circuit to represent the conductor arrangement. For basic circuit arrangements, this approach is adopted for live and protective earth conductors as in Fig. 12.

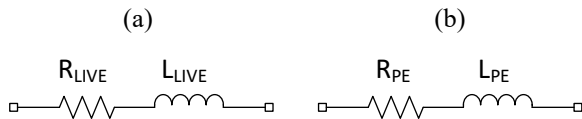


Fig. 12 Simplified short-circuit model: (a) live conductor; (b) protective earth (PE) conductor

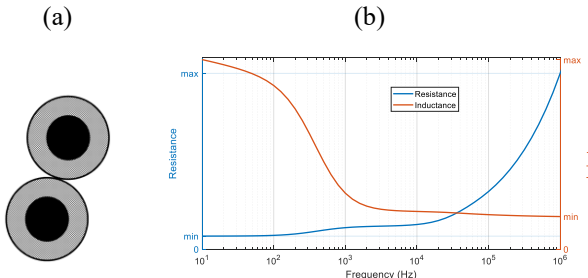


Fig. 13 Resistance (R) and inductance (L) trends: (a) basic cable arrangement; (b) R and L vs. frequency

While IEC 61660-1 [1] provides methods for determining per-unit-length parameters, care must be taken when using

models with fixed resistance and inductance values, as these do not account for frequency dependence. Computational results using [9] illustrate how resistance and inductance vary with frequency (see Fig. 13). As the physical arrangement can significantly influence mutual inductance, advanced methods should be employed for complex circuit arrangements to obtain accurate impedances. For improved accuracy, distributed-parameter models – potentially exhibiting frequency dependence – may be required.

3.2.4.2 Protective devices

The impedance of protective devices is normally neglected in prospective short-circuit current studies. However, it is deemed necessary to consider in certain cases when DC protective devices have an internal non-negligible inductor (L_{PDind}), with inherent resistance (R_{PDind}), to limit the current rate-of-rise. In this case, the device pole is modelled as a series resistor-inductor circuit (see Fig. 14), neglecting switching behaviour.

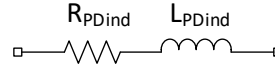


Fig. 14 Simplified short-circuit model: Protective device pole with non-negligible inductor

3.2.5 Short-circuit

A short-circuit is considered as an abnormal connection between live conductors of different potential, or a live conductor and an exposed-conductive-part or a protective conductor of different potential. While it may exhibit impedance in the real-world, it is modelled as a perfect (zero-impedance and instantaneous) short-circuit, or as close to this as the simulation framework allows e.g. modelled as a variable resistor, transitioning from 1 M Ω to $\leq 1\ \mu\Omega$ in one time-step.

3.3 Conditions

3.3.1 System configuration

The number of sources contributing to a short-circuit is not fixed and can vary with network configuration and operating conditions. To ensure realistic worst-case analysis, scenarios must account for changes such as equipment outages (e.g. during commissioning or maintenance), protective device operation altering the network state, reduced battery output at low state-of-charge, and diminished PV contribution under low irradiance.

For maximum and minimum short-circuit current, the configuration and operational mode that leads to the maximum and minimum value of prospective current at the short-circuit location, respectively, is proposed. For minimum short-circuit current, PV system contribution is proposed to be neglected.

3.3.2 Voltage levels

3.3.2.1 DC grid pre-fault voltage

Droop control is a strategy that can be implemented in active LVDC systems to balance power between sources and loads, resulting in voltage fluctuations during normal operation. IEC TR 63282 [2] defines voltage bands (B1 to B7), shown in Fig. 15, to ensure safe interoperability.

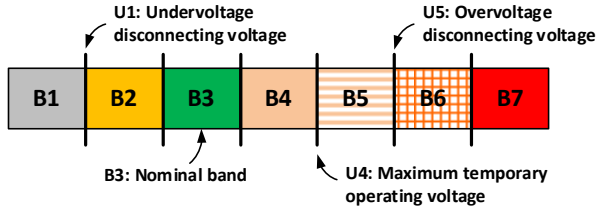


Fig. 15 IEC TR 63282 voltages bands

For maximum and minimum short-circuit current, the pre-fault voltage, defined by the nominal voltage, U_{DC} , and voltage factor, c_{DC} , is proposed to be U_4 and U_1 , respectively, for active LVDC systems using IEC TR 63282 voltage bands. For other (LV and MV) DC systems, the voltage is proposed to be at the maximum or minimum permitted voltage (excluding rapid transients), respectively.

3.3.2.2 AC supply system pre-fault voltage

To calculate AC system impedances (as outlined in Section 3.2.2.3), the corresponding voltage factors are required.

For maximum and minimum short-circuit current, the AC voltage is proposed to be equal to the voltage factor, c_{AC} , multiplied by the nominal line voltage, U_n , if IEC 60909 calculations are available. Otherwise, the AC voltage is proposed to be at the maximum or minimum permitted voltage (excluding rapid transients), respectively.

3.3.2.3 Battery pre-fault voltage

A battery is considered as either charged or discharged in relation to its nominal open-circuit voltage.

For maximum and minimum short-circuit current, the battery voltage is proposed to be equal to the voltage factor, c_{BATmax} or c_{BATmin} , respectively (with input from the battery manufacturer), multiplied by the nominal open-circuit battery voltage, U_{BAT} .

3.3.3 Component variation

Network component characteristics can vary due to operating conditions, environmental factors, and manufacturing tolerances. Accounting for possible variations is essential when determining short-circuit currents.

3.3.3.1 Conductor resistance

The DC resistance of a conductor is normally referenced at 20 °C. However, pre-fault resistance varies due to heating effects from load currents. The resistance at any temperature, T (in degree Celsius), can be calculated using Eq. (8), where $R_{T^{\circ}C}$ is the resistance at temperature T , $R_{20^{\circ}C}$ is the resistance at 20 °C, and α is a temperature coefficient equal

to 0.004/K, considered to have sufficient accuracy for common conductor materials [7] as shown in Fig. 16.

$$R_{T^{\circ}C} = R_{20^{\circ}C} \cdot [1 + \alpha \cdot (T - 20)] \quad (8)$$

For maximum short-circuit current, the pre-fault resistance is referenced at 20 °C. For minimum short-circuit current, it is referenced at the conductor's maximum sustained operating temperature (e.g. 90 °C for thermosetting insulation). Although PE conductor resistance should be evaluated separately, as it is not intended to carry load current and may be installed using various methods with differing temperature limits [10], the same approach is adopted. Resistance increase during the short-circuit is not considered.

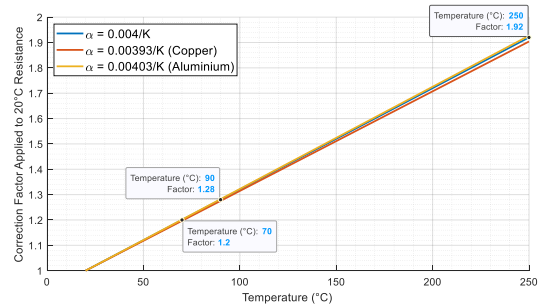


Fig. 16 Conductor resistance correction factors

3.3.3.2 Battery resistance

The battery resistance will depend on the state-of-charge, state-of-health, and cell temperature [6]. The effect of these dependencies will vary for different battery technologies however, a simpler approach is proposed.

For maximum and minimum short-circuit current, the battery resistance (R_{BAT}) is proposed to be modified to R_{BATmin} and R_{BATmax} , respectively, with input from the battery manufacturer.

3.3.3.3 Capacitance

Capacitor datasheets typically specify a $\pm 20\%$ capacitance tolerance [11]-[12], consistent with IEC 60384-4 [13] for electrolytic types, for instance. Further variation also arises from temperature, frequency, and cycling conditions [14].

For maximum and minimum short-circuit current, the capacitance is proposed to be 130 % and 70 %, respectively, of the nominal capacitance (C_C), incorporating the typical standard tolerance and an additional $\pm 10\%$ to simplify the estimation of other influencing factors.

3.3.3.4 Capacitor ESR

Capacitor datasheets typically specify ESR at a reference frequency and temperature (e.g. 100 Hz, 20 °C), though some manufacturers provide values under higher frequency and temperature conditions (e.g. 300 Hz, 60 °C), resulting in lower ESR values [11].

For maximum and minimum short-circuit current, the ESR is proposed to be taken as 30 % and 100 %, respectively, of the rated ESR (ESR_C) specified at ~ 100 Hz and ~ 20 °C.

This is based on a ratio between the ESR measured at different temperatures and frequencies [11].

3.3.3.5 Inductance

Understanding the saturation characteristics of an inductor is essential for accuracy. The inductor type significantly influences these characteristics; for instance, air-core inductors do not exhibit saturation, unlike iron-core types. Saturation behaviour can be classified as "soft" or "hard" depending on how inductance varies with higher current [15].

For maximum and minimum short-circuit current, the saturated inductance (L_{SAT}) and unsaturated inductance (L_{UNSAT}), respectively, are proposed to be used. If the saturation current is known and exceeded, L_{SAT} may be considered. A complete nonlinear model based on saturation characteristics ensures broader applicability.

3.3.3.6 Protective devices

DC protective devices may exhibit impedance and even contain an embedded inductor as described in Section 3.2.4.2. However, when the selection of semiconductor circuit-breakers and comparison with tested performance (i.e. a calibrated test circuit) is critical, special consideration is required.

To evaluate maximum short-circuit current – particularly the rate-of-rise to which the circuit-breaker is directly subjected – it is proposed that only the protective device immediately associated with the short-circuit be assumed to have zero impedance. Conversely, for minimum short-circuit current, the embedded inductor should be included. This approach results in prospective short-circuit currents that are dependent on the specific circuit-breaker(s).

3.3.4 Short-circuit locations

Careful selection of short-circuit locations is crucial for equipment specification, protection coordination, and selectivity, especially with bidirectional currents. For over-current protective devices, it is essential to determine both the maximum and minimum prospective currents. When short-circuit current sources exist on both sides of a protective device, short-circuit scenarios on each side must be evaluated. For maximum prospective current, the short-circuit must be located at the device terminals i.e. the source-end of the protected circuit(s). To assess the minimum prospective current, the short-circuit must be placed at the remote-end of the protected circuit(s).

3.4 Simulation

3.4.1 Configuration

Due to the presence of multiple sources in DC microgrids, numerous power flow scenarios are possible. Therefore, the system is modelled using only short-circuit contributors and impedances, neglecting pre-fault power flow. However, correction factors are applied to parameters influenced by power flow (see Section 3.3).

Once the model is configured with parameters adjusted for either maximum or minimum short-circuit current, initial conditions are set, and a short-circuit is introduced at the desired location. All voltage and current sources are initialised with their respective values, including pre-charged capacitors. A simulation time-step of 1 μ s is generally sufficient for most networks, offering a balance between accuracy and speed, though adjustments may be necessary depending on the model and simulation tool.

3.4.2 Outputs

Time-domain simulation outputs must align with general requirements such as those in [1], while accounting for emerging technologies and standards. The outputs proposed include the peak current magnitude from the instantaneous current value, steady-state current magnitude from the mean current value in the steady-state phase, and the current rate-of-rise ($\Delta i/\Delta t$) from the instantaneous current value obtained either at the onset of the short-circuit or at a defined level e.g. 63 % of the peak current (see Fig. 17). The rate-of-rise is critical for selecting semiconductor circuit-breakers, which are rated for a maximum allowable short-circuit current rise [16]-[17].

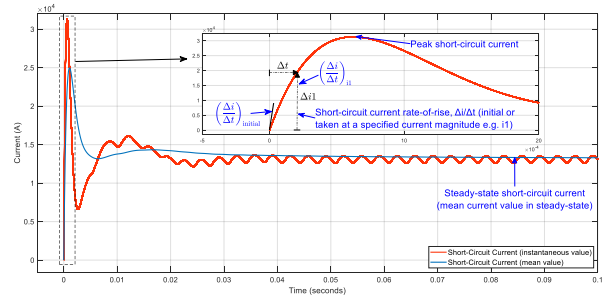


Fig. 17 Proposed short-circuit current outputs

4 Case Study

4.1 System

The proposed methodology, based on simplified short-circuit behavioural models, is applied to a two-wire DC microgrid comprising an AC grid with an AC/DC non-isolated InterLink 2-level converter, a battery with a bidirectional DC/DC non-isolated boost converter, a PV system with a unidirectional DC/DC non-isolated boost converter, and a DC/DC isolated single active bridge (SAB) converter supplying a sub-DC bus. Short-circuits are analysed in circuit 7 (1a and 1b) of the main DC grid and circuit 5 (2a and 2b) of the sub-DC grid, as shown in Fig. 18. Case -a represents a short-circuit at the source-end of the protected circuit, yielding maximum current, while case -b corresponds to the remote-end, resulting in minimum current.

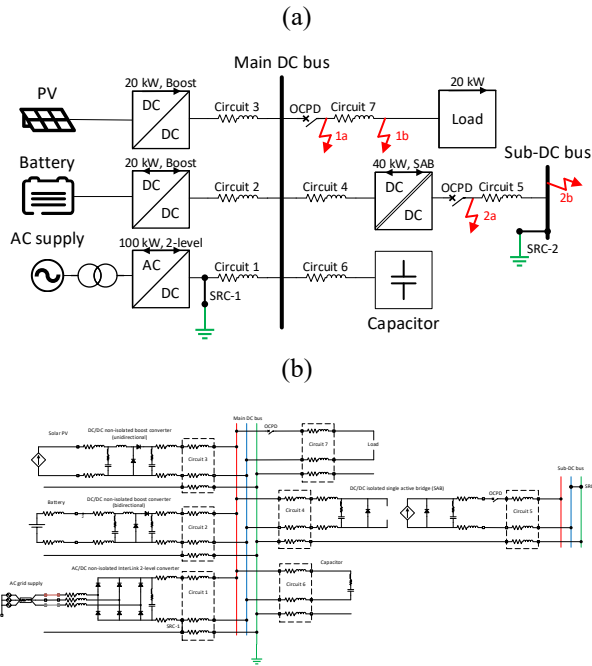


Fig. 18 DC microgrid diagrams: (a) basic single line diagram; (b) diagram using simplified behavioural models

System model parameters for each source, converter, and circuit are listed in Tab. 1. Both the main and sub-DC grids use a TN-S earthing arrangement, achieved by referencing the L- polarity to earth. The AC grid supply is isolated. The system-referencing conductor (SRC) is located near the AC/DC converter for the main DC grid and at the sub-DC bus for the sub-DC grid. Both grids are classified as low-voltage systems, designed in accordance with IEC TR 63282 voltage band specifications. The nominal voltage (U_{DC}) is 700 V, with a U4 voltage of 800 V ($c_{DCmax}=1.143$) and U1 voltage of 500 V ($c_{DCmin}=0.714$).

Model	Parameters
AC supply	$U_n=400$ V, $c_{ACmax}=1.1$, $c_{ACmin}=0.9$, $f_n=50$ Hz, $I''_{k3max}=10$ kA, $(X/R)_{k3max}=5$, $I''_{k3min}=6$ kA, $(X/R)_{k3min}=3$
Battery	$U_{BAT}=500$ V, $c_{BATmax}=1.05$, $c_{BATmin}=0.90$, $R_{BAT}=0.013$ Ω , $L_{BAT}=0.03$ mH
PV system	$I_{SC\ STC\ ARRAY}=30$ A, $K_f=1.25$, $U_{OC\ ARRAY}=600$ V
Capacitor	$C_c=0.005$ F, $ESR_c=0.005$ Ω , $ESL_c=Neglected$, $V_c=U_{DC} \times c_{DC}$
AC/DC converter	$R_{ACind}=4.25$ m Ω , $L_{ACindSAT}=200$ μ H, $L_{ACindUSAT}=680$ μ H, $C_c=10$ mF, $ESR_c=6.7$ m Ω , $ESL_c=30$ nH, $V_c=U_{DC} \times c_{DC}$, $R_{add}=2$ m Ω , $L_{add}=2$ μ H
DC/DC battery converter	Battery side: $C_c=10$ μ F; $ESR_c=7$ m Ω , $ESL_c=Neglected$, $V_c=U_{BAT} \times c_{BAT}$, $R_{add}=2$ m Ω , $L_{add}=2$ μ H, $L_{FSAT}=0.5$ mH, $L_{FUSAT}=Not\ considered$ Main DC grid side: $C_c=10$ μ F, $ESR_c=7$ m Ω , $ESL_c=Neglected$, $V_c=U_{DC} \times c_{DC}$, $R_{add}=2$ m Ω , $L_{add}=2$ μ H
DC/DC PV converter	PV system side: $C_c=10$ μ F; $ESR_c=7$ m Ω , $ESL_c=Neglected$, $V_c=U_{OC\ ARRAY}$, $R_{add}=2$ m Ω , $L_{add}=2$ μ H, $L_{FSAT}=0.5$ mH, $L_{FUSAT}=Not\ considered$ Main DC grid side: $C_c=10$ μ F, $ESR_c=7$ m Ω , $ESL_c=Neglected$, $V_c=U_{DC} \times c_{DC}$, $R_{add}=2$ m Ω , $L_{add}=2$ μ H

Model	Parameters
DC/DC SAB converter	Main DC grid side: $C_c=1.5$ mF, $ESR_c=65$ m Ω , $ESL_c=Neglected$, $V_c=U_{DC} \times c_{DC}$, $R_{add}=2$ m Ω , $L_{add}=2$ μ H Sub-DC grid side: $C_c=220$ μ F, $ESR_c=45$ m Ω , $ESL_c=Neglected$, $V_c=U_{DC} \times c_{DC}$, $R_{add}=2$ m Ω , $L_{add}=2$ μ H, $I_{SS-sc}=85$ A, $t_{SS-sc}=50$ ms
Circuits	Circuit 1: $R_{LIVEpul20^\circ C}=0.124$ m Ω /m, $R_{PEpul20^\circ C}=0.387$ m Ω /m, $L_{LIVEpul}=0.5$ μ H/m, $L_{PEpul}=0.5$ μ H/m, $l=20$ m Circuit 2-7: $R_{LIVEpul20^\circ C}=0.524$ m Ω /m, $R_{PEpul20^\circ C}=1.150$ m Ω /m, $L_{LIVEpul}=0.35$ μ H/m, $L_{PEpul}=0.35$ μ H/m, $l=30$ m
Protective devices	Zero impedance (without embedded inductor)

Tab. 1 System model parameters

The conditions used for determining maximum and minimum prospective short-circuit currents are given in Tab. 2.

Parameter	Maximum short-circuit current (case -a)	Minimum short-circuit current (case -b)
System configuration	All short-circuit contributors available and connected to the system.	For case 1b, only the AC supply and AC/DC converter. No change for case 2b.
DC grid voltage	$c_{DCmax} \times U_{DC} = 800$ V (U4)	$c_{DCmin} \times U_{DC} = 500$ V (U1)
AC voltage	$c_{ACmax} \times U_n = 440$ V	$c_{ACmin} \times U_n = 360$ V
Battery voltage	$c_{BATmax} \times U_{BAT} = 525$ V	Battery not connected.
Conductor resistance	Referenced at 20 $^\circ$ C	Referenced at 90 $^\circ$ C
Battery resistance	$R_{BATmin} = R_{BAT}$ (no adjustment applied)	Battery not connected.
Capacitance	$C_c \times 1.3$	$C_c \times 0.7$
ESR	$ESR_c \times 0.3$	$ESR_c \times 1.0$
Inductance	Saturated values (L_{SAT}).	Unsaturated values (L_{USAT}), otherwise L_{SAT} .

Tab. 2 Conditions applied to the case study

4.2 Results

Using the proposed methodology, the prospective currents are computed for both pole-to-pole (L+ to L-) and pole-to-earth (L+ to PE) short-circuits at each location. Results are presented in Tab. 3, with the rate-of-rise being the initial $\Delta i/\Delta t$ at short-circuit inception. Short-circuit current waveforms and mean current values for cases 1 and 2 are shown in Fig. 19 and Fig. 20, respectively.

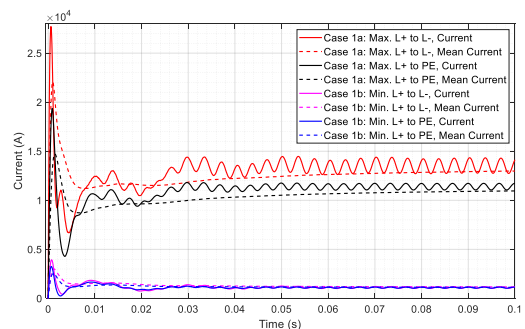


Fig. 19 Short-circuit current results: Case 1a and 1b

All waveforms initially exhibit a transient capacitor discharge (Stage 1). Subsequently, significant differences are observed: in case 1, a non-limiting AC/DC converter remains connected, resulting in prospective currents in the kiloamp range, even in the steady-state phase. In contrast, case 2 features SAB control of Stage 3 current, limiting it to approximately 1.5 p.u., equating to 85A (I_{SS-SC}), and disconnecting after 50 ms (t_{SS-SC}) for self-protection.

Short-circuit case	Peak current	Steady-state current	Initial rate-of-rise
1a: Max. L+ to L-	27.7 kA	13.0 kA	167.1 A/ μ s
1a: Max. L+ to PE	19.4 kA	11.0 kA	45.8 A/ μ s
1b: Min. L+ to L-	3.94 kA	1.17 kA	11.1 A/ μ s
1b: Min. L+ to PE	3.26 kA	1.13 kA	11.1 A/ μ s
2a: Max. L+ to L-	6.13 kA	Cut at 50ms	199.6 A/ μ s
2a: Max. L+ to PE	2.36 kA	Cut at 50ms	32.0 A/ μ s
2b: Min. L+ to L-	1.13 kA	Cut at 50ms	20.1 A/ μ s
2b: Min. L+ to PE	1.13 kA	Cut at 50ms	20.1 A/ μ s

Tab. 3 Short-circuit current simulation results

Variations between maximum and minimum short-circuit currents primarily result from differences in the number of contributing sources, the conditions applied to components (e.g. conductor resistance and capacitor parameters), and the short-circuit location. Differences between pole-to-pole and pole-to-earth short-circuits are attributed to the higher impedance of the PE conductor, further influenced by longer fault loops for some sources due to the positioning of the system-referencing conductor (SRC).

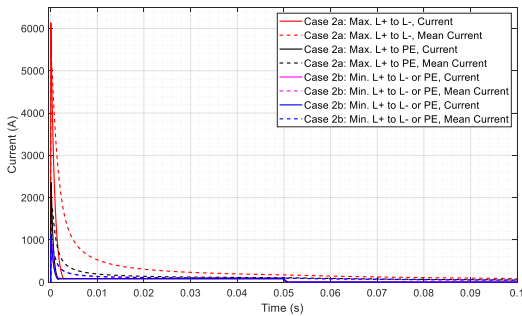


Fig. 20 Short-circuit current results: Case 2a and 2b

The current rate-of-rise for two short-circuit cases is presented in Fig. 21, illustrating both the continuous rate ($\Delta i/t$, assuming short-circuit initiation at time zero) and the incremental rate ($\Delta i/\Delta t$). This highlights significant differences between the initial rate-of-rise and that measured at a defined current level. In case 1a, the initial $\Delta i/\Delta t$ is approximately 167 A/ μ s, reducing to around 90 A/ μ s if taken at 63 % of the peak current. Aligning simulated current rate-of-rise values with the capabilities of semiconductor circuit-breakers is therefore critical.

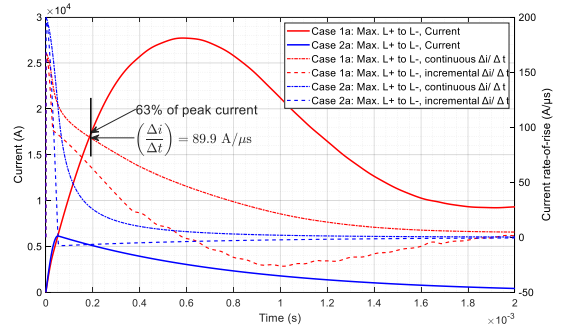


Fig. 21 Short-circuit current results: Rate-of-rise

5 Conclusion

This paper presents a comprehensive methodology for determining short-circuit currents in DC microgrids. The approach addresses shortcomings of the IEC 61660-1 standard, which is tailored to auxiliary installations and lacks coverage of common converter types, PV system contributions, accurate capacitor behaviour, and specificities of active LVDC systems. In the absence of validated analytical methods suitable for DC microgrids, the methodology relies on time-domain simulation using simplified short-circuit behavioural models, including those for power converters. Although this approach has some limitations, it offers a practical solution for engineering design by avoiding the complexities of detailed converter modelling and data acquisition, while maintaining sufficient accuracy. Moreover, the methodology is compatible with commercial transient analysis tools, enabling rapid and broad adoption to support the safe and efficient design of future DC microgrids.

Future work includes incorporating additional short-circuit contributors, enhancing the battery model for time-dependent behaviour, further analysing component variations including different capacitor types, assessing the need for additional outputs such as I^2t and root mean square (RMS) current, and validating the methodology with field data.

6 Acknowledgements

This research was supported in part by the European Union's Horizon Europe research and innovation programme under grant agreement no. 101136131. Views and opinions expressed in this document are those of the authors only and do not necessarily reflect those of the European Union or the European Climate, Infrastructure and Environment Executive Agency. Neither the European Union nor the granting authority can be held responsible for them.

7 References

- [1] IEC 61660-1:1997, First edition 1997-06, *Short-circuit currents in d.c. auxiliary installations in power plants and substations – Part 1: Calculation of short-circuit currents.*

- [2] IEC TR 63282, Edition 2.0 2024-08, *LVDC systems – Assessment of standard voltages and power quality requirements*.
- [3] J.J. Deroualle, D. Pescatori, A. Dellacasa, C. Davico, “Comparison of short-circuit current calculations in DC shipboard power system for Fuse protection designing”, *Electric Power Systems Research*, vol. 199, 2021, 107353, ISSN 0378-7796, <https://doi.org/10.1016/j.epsr.2021.107353>.
- [4] S. Beheshtaein *et al.*, “DC Microgrid Protection: A Comprehensive Review,” in *IEEE Journal of Emerging and Selected Topics in Power Electronics*.
- [5] Ming Yu *et al.*, “DC short circuit fault analysis and protection of ring type DC microgrid,” *2016 IEEE 8th International Power Electronics and Motion Control Conference (IPEMC-ECCE Asia)*, Hefei, China, 2016, pp. 1694-1700.
- [6] SeaZero, Project Report, Review of Methods for Battery Systems External Short-Circuit Calculations, Task 2.1, Deliverable 2.1.1, Report Number 2023:00713—Unrestricted.
- [7] IEC 60909-0, Edition 2.0 2016-01, *Short-circuit currents in three-phase a.c. systems – Part 0: Calculation of currents*.
- [8] IEC 60364-7-712, Edition 2.0 2017-04, *Low voltage electrical installations – Part 7-712: Requirements for special installations or locations – Solar photovoltaic (PV) power supply systems*.
- [9] Amauri Martins-Britto (2025). LineCableLab (<https://github.com/amaurigmartins/LineCable-Lab/releases/tag/7.0.3>), GitHub. Retrieved January 21, 2025.
- [10] IEC 60364-5-54 COMPIL:2021, *Low-voltage electrical installations – Part 5-54: Selection and erection of electrical equipment – Earthing arrangements and protective conductors*.
- [11] TDK Electronics AG, "B43703, B43723 Aluminum Electrolytic Capacitors Datasheet," [Online]. Available: https://www.tdk-electronics.tdk.com/inf/20/30/db/aec/B43703_B43723.pdf. [Accessed: Jul. 16, 2025].
- [12] Vishay Intertechnology, Inc., "299PHL4TSI High Voltage Snap-In Capacitors Datasheet," [Online]. Available: <https://www.vishay.com/docs/28432/299phl4tsi.pdf>. [Accessed: Jul. 16, 2025].
- [13] IEC 60384-4:2016, 2016-08, *Fixed capacitors for use in electronic equipment – Part 4: Sectional specification – Fixed aluminium electrolytic capacitors with solid (MnO₂) and non-solid electrolyte*.
- [14] TDK Electronics AG, "General technical information – aluminum electrolytic capacitors," [Online]. Available: <https://www.tdk-electronics.tdk.com/download/185386/e724fb43668a157bc547c65b0cff75f8/pdf-generaltechnicalinformation.pdf>. [Accessed: Jul. 16, 2025].
- [15] Vishay Intertechnology, Inc., "Did you know? IHLP® inductors and saturation current," [Online]. Available: https://www.vishay.com/docs/48155/_did-you-know_ihlp_saturation_vmn-ms7373.pdf. [Accessed: Jul. 16, 2025].
- [16] IEC CDV 60947-10 (121A/635/CDV), *Low-voltage switchgear and controlgear – Part 10: Semiconductor Circuit-Breakers*.
- [17] Underwriters Laboratories Inc. (UL). UL Standard for Solid State Circuit Breakers, UL 489i, Northbrook, IL 60062-2096 (Draft comments due April. 12, 2024).